Aerosol transmission risk of COVID-19 when passengers move slowly in a line at the airport terminal

Yu Zhao[1*], *Yao Feng*[1]

[1]Dalian University of Technology, China

Abstract. The airport terminal with high numbers of occupied passengers has potentially become high risk region for aerosol transmission of COVID-19. In this paper, the Eulerian-Lagrangian approach and realizable k–ε turbulence model is used to numerically simulate the airflow organization and aerosol transmission when passengers move slowly in a line. During the aerosol transmission period, evaporation is also enrolled as it is a key factor influencing particle size distribution at the beginning of aerosol transmission from the human. In addition, the process of passenger moving in the airport terminal is realized by employing dynamic mesh algorithms. The results of the study show that people who are behind the infected person during the queuing movement have a higher risk of infection than those who are in front. In addition, the disturbance of people walking has an important influence on the distribution of aerosols.

* Corresponding author: zhaoyu1220@dlut.edu.cn

1 Introduction

The airport terminal with high numbers of occupied passengers has potentially become high risk region for aerosol transmission of COVID-19. Recent studies [1-3] mostly focused on airflow patterns and aerosol transmission risk at the seating and standing situations [4] of commuters inside the traffic-related environment, e.g. subway, coach bus, airplane, airport terminal, etc. In the public environment, safe social distancing is also a key in the study [5]. This proves that many researchers are aware of the risk of aerosol transmission in Covid-19 and has made some basic research. However, for most public environments, personnel is a factor that cannot be ignored, especially when queuing and luggage boarding are common scenarios at the airport. Through the phenomenon of traffic wind formed in the process of vehicle movement, especially under low speed conditions, we believe that the movement of people must also cause disturbance to the surrounding environment. Although some scholars have studied the diffusion of pollutants in personnel walking [6-7], there is little research on this aspect.

Thus, the aims of the studies are to extract the quantitative description of aerosol transmission risk of COVID-19 under passenger moving conditions, combining a Realizable k-ε model, Eulerian-Lagrangian approach and dynamic mesh technique. The particles exhaled by the human body are 50-micron droplets. The study could be a guidance of personal protection for passengers and optimized ventilation control at the airport terminals.

2 Methods

2.1 Numerical simulation airflow model and droplet mode

The Realizable k-ε model with all y+ Wall Treatments were employed to simulate the turbulent flow inside the airport terminal. Lagrangian method was used to track respiratory droplets. This approach calculates the trajectory of each droplet by solving the individual droplet movement equation whose theory is Newton's second law:

$$\frac{du_{pi}}{dt} = \sum F_i = F_{drag,i} + F_{g,i} + F_{a,i} \quad (1)$$

where upi is droplet velocity in the i direction (m/s), ∑Fi is the sum of all external forces exerted on the droplet (per unit droplet mass) in i direction (m/s2). The external forces consist of the drag force, Fdrag,i, the gravity Fg,i and the additional forces Fa, i.

Respiratory droplets are composed of 90 % liquid (water) and 10 % solid elements (sodium chloride), coinciding with Potter et al. 1963 [8]. The densities of water liquid and sodium chloride are 1000 kg m−3 and 2170 kg m−3, respectively. The density of the droplet followed the volume weighted mixing law. The specific heat followed the mass weighted mixing law. The droplet vaporization rate is defined as the following equation:

$$\dot{m}_p = -\varepsilon_i g^* A_s ln(1 + B) \quad (2)$$

Where, the sequential number i refers to each component in the mixed component; ε_i is the fractional mass transfer rate; B is the number of Spalding transfers, indicating the driving force of evaporation; g* is the mass transfer conductance.

2.2 Geometry model

In this study, we established a geometric model to simulate a common check-in or boarding scenario in airports. The dimensions of the geometric model in the X, Y, and Z directions are 10m, 20 m, 10 m, respectively. According to the common ventilation mode of the airport check-in hall, we have set up the ventilation mode of up-supply and down-return with different sides along the -Y direction. The air supply inlet is a circular nozzle with a diameter of 500 mm placed 3.5 m from the ground, while the return air outlets are 1500 mm × 650 mm louver return air vents placing 0.5 m from the ground. Five standing human models are placed in the Y direction (air supply direction) for movement. According to the common scenes of queuing and moving slowly during passenger boarding and luggage check-in at the airport terminal, we set two conditions for calculation: (1) walking in the leeward direction: personnel move along the direction of the air supply vent (minus Y direction); (2) walking in the windward direction: Personnel move against the direction of the air supply vent (positive Y direction).

For passengers in the terminal, we established a 1:1:1 geometric model according to the standing size of adults. The height of the human body is approximately 1.7 m, the length of the head is approximately 0.37 m, the maximum head radius is 0.17 m, and the length of the upper body is approximately 0.7 m. The nose is simplified as two circles with r = 0.005 m, and the mouth is simplified as an ellipse with a primary radius of 0.03 m and a secondary radius of 0.02 m.

The geometric and human body models are shown in Fig. 1.

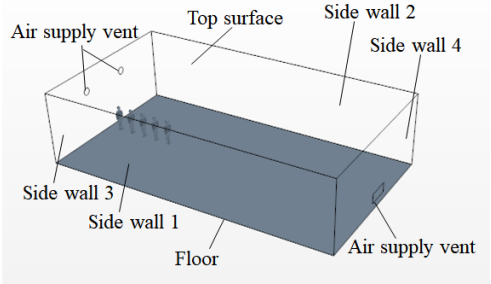

(a) The geometric model of walking in the leeward direction

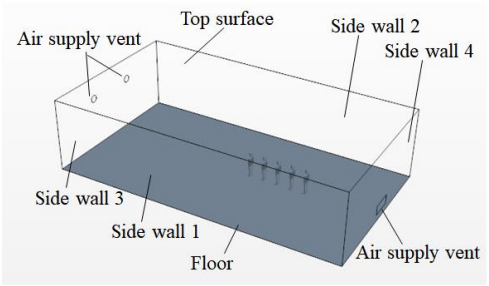

(b) The geometric model of walking in the windward direction

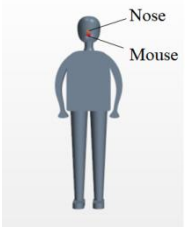

(c) The human body model

Fig. 1. Geometric and human body models

2.3 CFD mesh establishment and simulation conditions

After the model was established, it was necessary to mesh the model. The speed, precision, and convergence of the simulation calculations are closely related to the quality of the mesh. In this study, STAR-CCM+ software was used to mesh the model. The mesh model used was an unstructured mesh and was used for the surface reconstruction. The mesh generator included a polyhedral mesh generator and a prism-layer mesh generator. The basic size of the grid was 0.1 m, and custom grid sizes were set in specific areas, such as the air supply outlet, return air outlet, and surface of the human body, for encryption.

All boundary conditions for airflow are summarized in Table 1. In the study, we set the human walking speed to 1 m/s. The influences of human breathing and heat flux at body surfaces were taken into the account. In a state of extremely light work, just like people in the office, hotel or waiting hall, the human body releases about 134W of heat. The ratio of radiation, convection and latent heat is 40%, 20%, and 20%, respectively [9]. The surface area of the human body is approximately 1.6-2.0 m^2. Thus, the human body was set to have a constant heat flow boundary of 71.7 W/m^2. Talking is a more common behaviour than coughing and sneezing. In the study, we assumed an example of an infected person who has been talking and exhaling aerosols, so we set the exhalation speed of the human mouth to be 1.08 m/s, and the nose inhales with a constant pressure of -0.754 Pa [10]. Non-slip boundary conditions were applied for all walls where isothermal condition was assumed.

Table 1. Boundary conditions for airflow simulation.

Boundary name	Boundary conditions
Air supply vent	velocity inlet, velocity is 3.72 m/s, temperature equals to 18 ℃,
Air return vent	Pressure exit, pressure is -2.083 Pa
Mouths	velocity inlet, velocity is 1.08 m/s, temperature equals to 34 ℃,
Noses	Pressure exit, pressure is -0.754 Pa
Body surface	standard wall function, no slip wall, heat flux is 71.7 W/m^2
Floor， Top surface, Side wall	standard wall function, no slip wall

Droplets were injected into the space through the mouth of the patient at a rate of 860 drops / s. The Discrete Phase Boundary Conditions (DPBC) type was summarized in Table 2. For floor, body surfaces and side walls, the quit condition was applied with the assumption that droplets were deposited as soon as they touch the wall surfaces and the trajectory calculation was terminated. Escape condition was applied to the nose and mouths as well as air-conditioning vents.

Table 2. Boundary conditions in simulations of droplet dispersion (discrete phase).

Boundary name	Boundary conditions
Air supply vent, Air return vent, mouths, noses	Escape (trajectory calculations are terminated here)
Side wall, Top surface, Floor, Body surface	Quit (trajectory calculations are terminated here)

3 Results and discussion

3.1 Aerosol distribution field

In the two states of walking in the leeward direction and walking in the windward direction, we assume that the person in the middle of the five people is an infected patient and will continuously exhale aerosol particles during the walking process. We calculated the diffusion motion of the aerosol for 10 seconds during the movement of people. The calculation results at the 5th and 10th seconds are as follows:

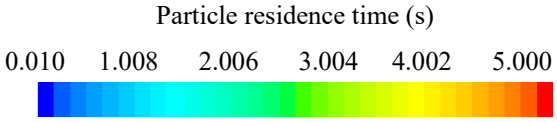

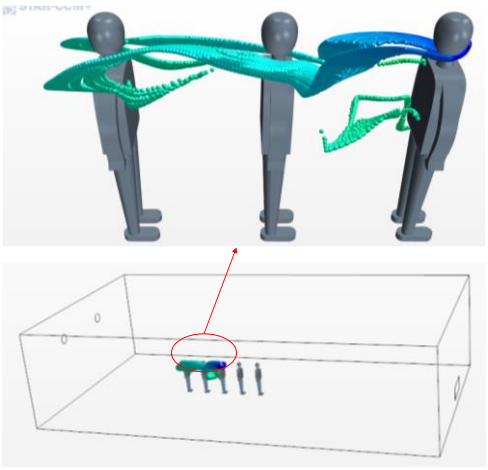

(a) Aerosol distribution in second 5

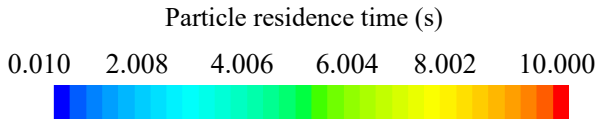

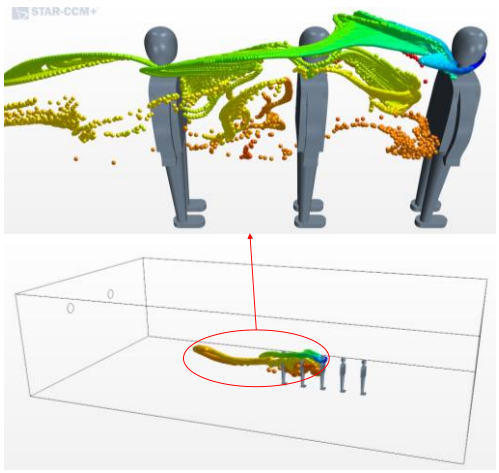

(b) Aerosol distribution in second 10

Fig. 2. Aerosol distribution in the leeward direction

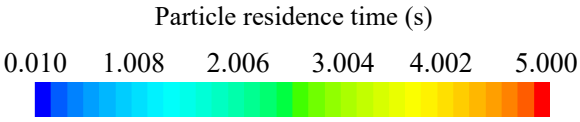

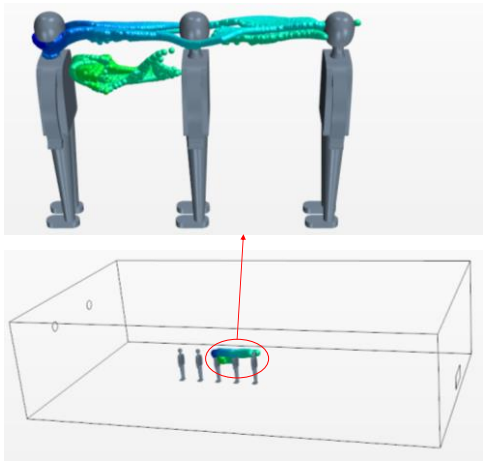

(a) Aerosol distribution in second 5

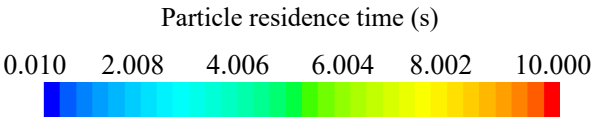

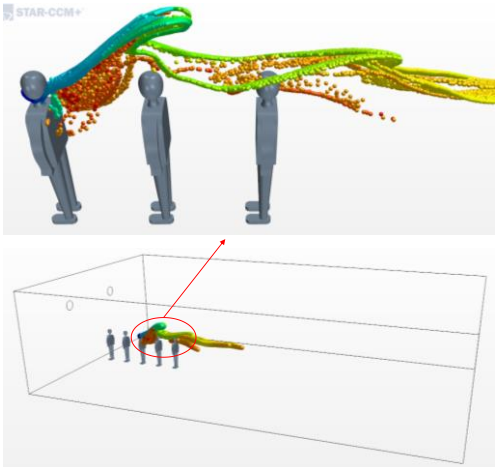

(b) Aerosol distribution in second 10

Fig. 3. Aerosol distribution in the windward direction

By comparing the aerosol distribution characteristics at the 5th and 10th seconds, it can be clearly seen that the diffusion range of the aerosol increases with the movement of the person. At the same time, the aerosol distribution in the 10th second is more dispersed than that in the 5th second, which indicates that the aerosols exhaled by people are affected by the air flow formed by the environment and people's walking.

We found that there is a greater risk of infection for those behind the infected person and almost no risk for those in the front during a person's walking, which is the exact opposite of what we usually think of people in the front as being more susceptible. As the person moves, the virus-laden aerosol is left behind the infected person and spreads under the influence of the airflow. For the two situations, the figure shows that the aerosol near the person is more dense when walking in the leeward direction, possibly because the direction of the person walking is the same as the wind direction, which causes the aerosol to gather near the human body under the influence of airflow.

3.2 Aerosol Diffusion Distance

Since the geometric model developed in this study was located at 0 – 20 m in the + Y direction, we counted the farthest distance of aerosol particles in the Y direction from the infected person, as shown follows.

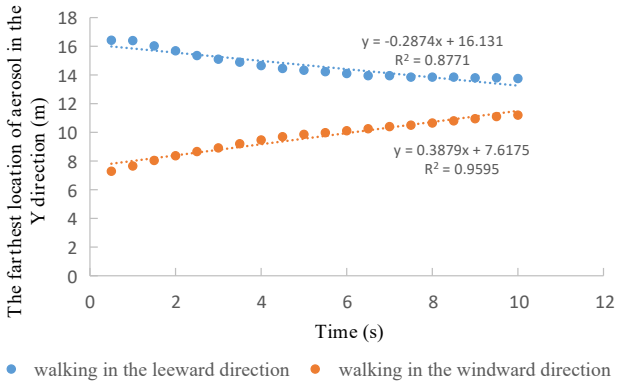

Fig. 4. The farthest distance for aerosol diffusion in the *Y* direction

From the chart, we can see that no matter whether the person walk leeward or windward, the aerosol moves forward with the person's walking direction, indicating that the disturbance formed by the person's walking indeed has an important impact on the distribution of aerosol. In addition, as the person gradually moves forward, the farthest position of the aerosols changes less and less, perhaps the aerosol may eventually gather within a certain range during the movement of the person.

A linear relationship is approximated by analyzing the variation of the farthest propagation position of the particle diffusion with time. In addition, we counted the farthest distance from the human mouth that the particles diffused after 10 seconds. The results showed that the particles diffused 6.84m in leeward walking, and 6.89m in windward walking.

4 Conclusions

According to the analysis of the aerosol distribution during the dynamic movement of people, we can draw the following conclusions: people who are behind the infected person during the queuing movement have a higher risk of infection than those who are in front; The disturbance of people walking has an important influence on the distribution of aerosols. The farthest propagation position of the particle diffusion varies with time approximately linearly. After a person walks for 10 seconds, the farthest distance of the particle diffusion from the human mouth can reach 6.89m.

References

1. M. Jayaweera, H. Perera, B. Gunawardana, J. Manatunge, Transmission of COVID-19 virus by droplets and aerosols: A critical reviewon the unresolved dichotomy, Environ. Res. **188**, 109819 (2020)
2. X. Yang, C.Y. Ou, H.G. Yang, L. Liu, T. Song, M. Kang, H.L. Li, J. Hang, Transmission of pathogen-laden expiratory droplets in a coach bus, J. Hazard. Mater. **397**, 122609 (2020)
3. L. Zhang, Y.G. Li, Dispersion of coughed droplets in a fully-occupied high-speed rail cabin, Build. Environ. **47**, 58-66 (2012)
4. N. Sen, Transmission and evaporation of cough droplets in an elevator: Numerical simulations of some possible scenarios, Phys. Fluids. **33**, 033311 (2021)
5. T. Dbouk, D. Drikakis, On coughing and airborne droplet transmission to humans, Phys. Fluids **32**, 053310 (2020)
6. J. Hang, Y.G. Li, R.Q. Jin, The influence of human walking on the flow and airborne transmission in a six-bed isolation room: Tracer gas simulation
7. S. Mazumdar, S.B. Poussou, C.H. Lin, S.S. Isukapalli, M.W. Plesniak, Q.Y. Chen, Impact of scaling and body movement on contaminant transport in airliner cabins, Atmos. Environ. **45**, 6019e28 (2011)
8. J. L. Potter, L. W. Matthews, J. Lemm, S. Spector, Human pulmonary secretions in health and disease, Ann. NY. Acad. Sci. **106 (2)**, 692-697 (1963)
9. R. Y. Zhao, C. Y. Fan, D. H. Xue, Y. M. Qian, Air Conditioning, fourth ed., China Architecture & Building Press China, 2009.
10. J. K. Gupta, C. Lin, Q.Y. Chen, Characterizing exhaled airflow from breathing and talking, Indoor. Air. **20**, 31-39 (2010)